

Fractal conduction pathways governing ionic transport in a glass

J. L. Iguain

*Instituto de Investigaciones Físicas de Mar del Plata (IFIMAR) and Departamento de Física FCEyN,
Universidad Nacional de Mar del Plata - Deán Funes 3350, 7600 Mar del Plata, Argentina.*

F. O. Sanchez-Varreti

Universidad Tecnológica Nacional - Facultad Regional San Rafael (FRSR) – SiCo.

M. A. Frechero

*INQUISUR-UNS-CONICET and Departamento de Química Universidad Nacional del Sur - Avenida Alem 1253,
8000 Bahía Blanca, Argentina.*

We present a systematic characterization of the fractal conduction pathways governing ionic transport in a non-crystalline solid below the glass-transition temperature. Using classical molecular dynamics simulations of lithium metasilicate, we combine mobility-resolved dynamical analysis with a real-space description of the regions explored by lithium ions. Ensemble-averaged velocity autocorrelation functions rapidly decorrelate and do not resolve the pronounced dynamic heterogeneity of the system, whereas single-ion analysis reveals short-lived episodes of nearly collinear motion. By mapping active-site clusters over increasing time windows, we show that ion-conducting pathways are quasi one-dimensional at short times and evolve into larger, branched structures characterized by a robust fractal dimension $d_f \simeq 1.7$. This geometry persists while the silicate backbone remains structurally arrested, whereas near the glass-transition temperature the loss of structural memory leads to the reappearance of small clusters. These results provide a real-space structural interpretation of ionic transport in non-crystalline solids and support fractal pathway models of high-frequency ionic response.

PACS numbers: 66.30.H-, 61.43.Hv

The Universal Dielectric Response (UDR), also known as Jonscher's law, provides a unifying description of the AC electrical response of a wide variety of materials exhibiting relaxation and conduction phenomena. Originally proposed by Jonscher in 1977 [1], this empirical law captures the frequency dependence of the AC conductivity $\sigma(\omega)$ observed in many dielectrics and semiconductors, particularly in structurally disordered systems. Its broad applicability suggests the existence of a common underlying charge-transport mechanism operating across diverse classes of materials.

For the real part of the complex conductivity, Jonscher's law is commonly written as

$$\sigma'(\omega) = \sigma_{\text{DC}} + A\omega^n, \quad (1)$$

where $\sigma_{\text{DC}} = \sigma'(\omega \rightarrow 0)$ is the DC conductivity, A is a temperature-dependent prefactor, ω is the angular frequency, and n is the Jonscher exponent, typically in the range $0 < n \leq 1$. The value of n provides insight into the dominant transport mechanism: small values correspond to nearly frequency-independent conduction, while increasing n reflects correlated hopping processes and stronger interactions between charge carriers and the surrounding matrix. In the limiting case $n = 1$, the response approaches ideal Debye behaviour, characteristic of non-interacting dipoles with a single relaxation time.

The essential difference between Jonscher's law and the classical Debye model lies in the complexity of the relax-

ation dynamics they describe. In disordered materials, charge carriers are localized in a broad distribution of energy wells and must hop between sites to contribute to transport. At low frequencies, carriers can explore long distances, giving rise to DC conduction. At higher frequencies, the rapidly oscillating field restricts motion to short-range, localized displacements [2, 3]. While such motion contributes weakly to long-range transport, it strongly enhances dielectric losses, leading to the characteristic power-law increase of the AC conductivity [4–6]. Jonscher's law effectively captures this correlated, multi-scale dynamics through an implicit distribution of relaxation times, in contrast to the single-time-scale dynamics assumed in the Debye model.

Ionic glasses represent a paradigmatic class of materials exhibiting Universal Dielectric Response. Their intrinsic structural disorder arises from a covalent glassy network within which mobile ions act as charge carriers. These ions experience a complex and heterogeneous energy landscape, characterized by a broad distribution of site energies and hopping barriers that are neither spatially uniform nor dynamically equivalent [4, 5, 7, 8]. Despite extensive experimental and computational efforts, a complete microscopic understanding of ionic transport in these systems remains elusive.

A recurring concept in this context is that of ion-conducting pathways: preferential regions of enhanced mobility embedded within the disordered structure. Dif-

diffusive transport in non-crystalline systems has long been associated with such regions, which were anticipated as near-one-dimensional, fractal objects well before they could be directly resolved. Clarifying their geometry, temporal stability, and contribution to macroscopic transport remains a central challenge, requiring the analysis of ion dynamics across multiple spatial and temporal scales [9–12].

In this work, we investigate a lithium metasilicate glass from a microscopic perspective, focusing on the temporal evolution of lithium-ion dynamics in the presence of strong dynamic heterogeneity. Our primary objective is to identify and characterize the ion-conducting pathways explored by the most mobile ions, determine their geometrical properties, and establish a direct connection with the high-frequency regime of the AC ionic conductivity, corresponding to short times and limited spatial exploration. By linking microscopic ion dynamics to macroscopic dielectric response, this study provides new insight into the structural origin of transport anomalies in ion-conducting glasses and contributes to the rational design of non-crystalline solid-state electrolytes.

Numerical simulations.- To investigate the evolution of lithium-ion dynamics upon approaching the glass transition from the liquid state, we focus on lithium metasilicate (Li_2SiO_3), a model ion-conducting glass that has been extensively studied in the literature. Previous analyses [13, 14] have reported pronounced temperature-dependent effects in this system, particularly in the mobility of lithium ions within the glassy network, providing valuable insight into transport mechanisms near the glass transition.

The system consists of 3456 atoms, corresponding to the Li_2SiO_3 stoichiometry, and is modelled using classical molecular dynamics simulations. Interatomic interactions are described by a Gilbert–Ida-type pair potential [15], which includes long-range Coulomb interactions with effective charges, a dispersive r^{-6} term acting between oxygen ions, and a short-range Born–Mayer repulsive contribution. The interaction parameters were taken from previous studies and validated for this system [16–18] through ab initio molecular orbital calculations.

Atomic velocities were initially assigned according to a Maxwell–Boltzmann distribution at 3500 K. The system was first equilibrated at this temperature for 2 ns in the microcanonical (NVE) ensemble. It was then cooled to the target temperatures of 700 K and 1100 K using an identical quench rate in all cases. Cooling was performed in two consecutive stages, each consisting of a 2 ns simulation in the isothermal–isobaric (NPT) ensemble, during which a thermostat imposed a linear decrease in temperature while maintaining the pressure at 1 atm. At each target temperature, an additional 2 ns NPT equilibration was carried out to ensure thermal stability and to attenuate pressure fluctuations typical of solid phases. The corresponding experimental densi-

ties were reproduced within reported uncertainties. From the temperature dependence of the system volume, the glass-transition temperature was identified as $T_g = 1200$ K [13, 14].

The equations of motion were integrated using the Verlet algorithm with periodic boundary conditions and a time step of 1 fs, as implemented in the LAMMPS simulation package [19]. Production trajectories were generated in the NPT ensemble. For subsequent analysis, 101 configurations were extracted from each trajectory at intervals of 200 fs, ensuring statistical independence while avoiding significant structural relaxation effects [20].

Autocorrelation function.- The velocity autocorrelation function $Z(t)$ (VACF)

$$Z(t) = \frac{\sum_i |\mathbf{v}_i(t) \cdot \mathbf{v}_i(0)|^2}{\sum_i |\mathbf{v}_i(0) \cdot \mathbf{v}_i(0)|^2} \quad (2)$$

is the standard tool for linking microscopic dynamics with transport properties in disordered ionic systems. It provides key information about the temporal evolution of ionic motion and is typically interpreted through four features: (i) an initial rapid decay associated with vibrational motion within the transient oxygen cage (femtosecond–picosecond scale); (ii) a negative minimum (backscattering), common in liquids and disordered solids, where an ion reverses direction after colliding with neighbours; (iii) a long-time decay to zero, signalling the onset of diffusive motion; and (iv) its direct relation to the diffusion coefficient via the Green–Kubo formula. Accordingly, the VACF is widely used to probe relaxation processes and microscopic transport, including dynamical changes across the glass transition [21–23].

To investigate dynamic heterogeneity, we focus on the lithium ions, the most mobile species in the system. A segmentation procedure is applied in which all Li atoms are first considered, and a mobility criterion is introduced: ions whose positional standard deviation exceeds 1Å are classified as fast, whereas the remaining ions are labelled slow [13].

This procedure yields two mobility-resolved subsets at fixed temperature. The VACF is then computed separately for the fast and slow lithium ions and compared with the VACF averaged over all Li^+ . Our working hypothesis is that fast ions should exhibit a more rapid loss of velocity correlation, characterized by reduced backscattering and a faster decay to zero, consistent with weaker confinement by the oxygen network and a more liquid-like local environment.

Figure 1 shows the VACFs computed for the full lithium ensemble and for the two mobility subsets at temperatures below the glass transition. In all cases, the VACF decorrelates within only a few timesteps, indicating that ensemble-averaged velocity correlations are largely insensitive to the pronounced dynamic heterogeneity reported previously [2, 24]. A more detailed

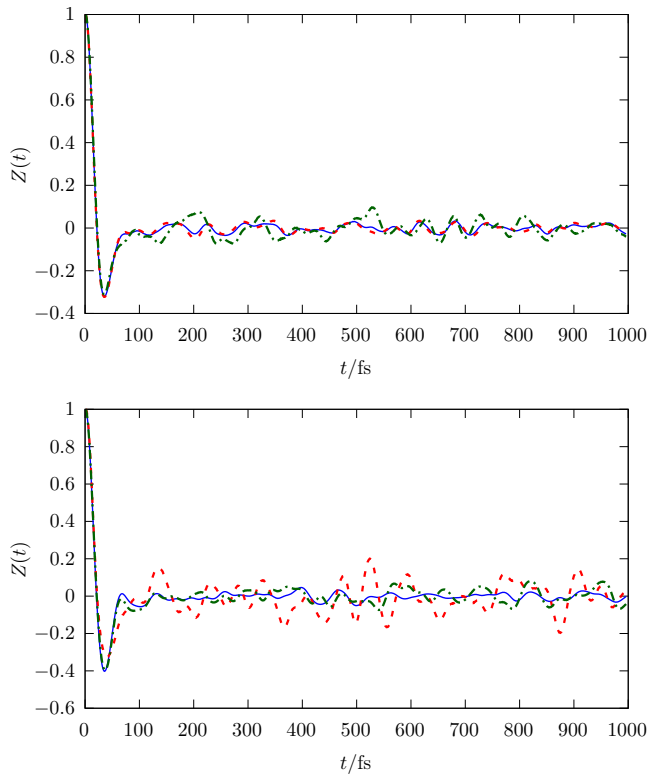


FIG. 1. (color online) Lithium velocity autocorrelation function as a function of time for two temperatures: 1000 K (top) and 700 K (bottom). In each panel, the dashed (red) line corresponds to fast ions, the dash-dotted (green) line to slow ions and solid (blue) line to the ensemble average

picture emerges when the analysis is carried out at the level of individual ions. In this case, the VACFs exhibit intermittent episodes in which they approach values close to unity, signalling nearly collinear motion over short time intervals. These events provide direct evidence of transient, less-restricted displacements along preferred directions, consistent with the existence of ion-conducting pathways. Importantly, such episodes occur asynchronously across different ions and are therefore strongly suppressed by ensemble averaging. Furthermore, although the most mobile ions explore extended, three-dimensional trajectories, the directional correlations associated with these motions are effectively washed out when averaged over the full ensemble. As a consequence, the geometric signature of the conduction pathways remains hidden in conventional VACF analyses. Taken together, these results show that ensemble-averaged VACFs, despite their widespread use, do not resolve the structural features of the diffusive pathways governing ionic transport in non-crystalline solids. This motivates the spatially resolved pathway analysis presented next.

Pathway structure.-

Having established that ensemble-averaged velocity

correlations are unable to resolve dynamic heterogeneity, while single-ion VACFs reveal short-lived episodes of nearly collinear motion, we now turn to the spatial origin of this behaviour. If highly mobile ions undergo transient intervals of directed motion, this must be reflected in the geometry and connectivity of the regions they explore. We therefore analyse the structure of the ion-conducting pathways, with the aim of identifying the spatial organisation that supports these less-restricted displacements.

To this end, the simulation box is discretized into a cubic grid of approximately 200 sites per side. All sites are initially marked as inactive; a site becomes active as soon as it is visited by any lithium ion. As the simulation evolves, the number of active sites increases, forming clusters whose structure reflects the regions explored by ionic motion. Below the glass-transition temperature, the silicate network formed by silicon and oxygen atoms is highly rigid. As a result, the conduction pathways are expected to remain stable over time windows sufficiently long for the incoherent scattering function to remain close to unity [25, 26].

Lithium ions explore the system by performing random walks constrained by this network of conductive channels. Accordingly, the ion-conduction pathways can be inferred from the geometry of the clusters formed by active sites. Two limiting cases can be identified: ions confined to very small clusters remain localized near their initial positions, whereas ions belonging to large, percolating clusters are able to contribute to long-range electrical conduction. More generally, each cluster contributes to the electrical response on characteristic length and time scales determined by its size and morphology.

To characterize the temporal evolution of the conduction pathways, we systematically evaluated, at regular time intervals, the size M of each active-site cluster (number of active sites), its spatial extent l (maximum pairwise distance), and its box-counting fractal dimension d_f . Figure 2 shows representative clusters containing more than 300 active sites for the system at $T = 700$ K at three different times ($t = 5, 10, \text{ and } 15$ ps).

We first analysed the statistical properties of the conduction clusters at $T = 700$ K for times $t = 1, 2, 4, 6, 10, 15, 20$ and 30 ps. As shown previously [25, 27], the incoherent scattering function remains close to unity over this time window, indicating that the silicate backbone remains essentially stable. The evolution of the fractal dimension as a function of cluster length is shown in Fig. 3 (top). At short times, most clusters are small and exhibit fractal dimensions close to $d_f \simeq 1$, indicating that, at small spatial scales, the conducting pathways are quasi one-dimensional. As time progresses, some clusters grow and merge, forming larger structures, while others saturate and cease to evolve. The larger clusters display a nearly constant fractal dimension close to $d_f \simeq 1.7$, signalling the emergence of a branched, fractal geometry.

This behaviour is further illustrated in Fig. 3 (bot-

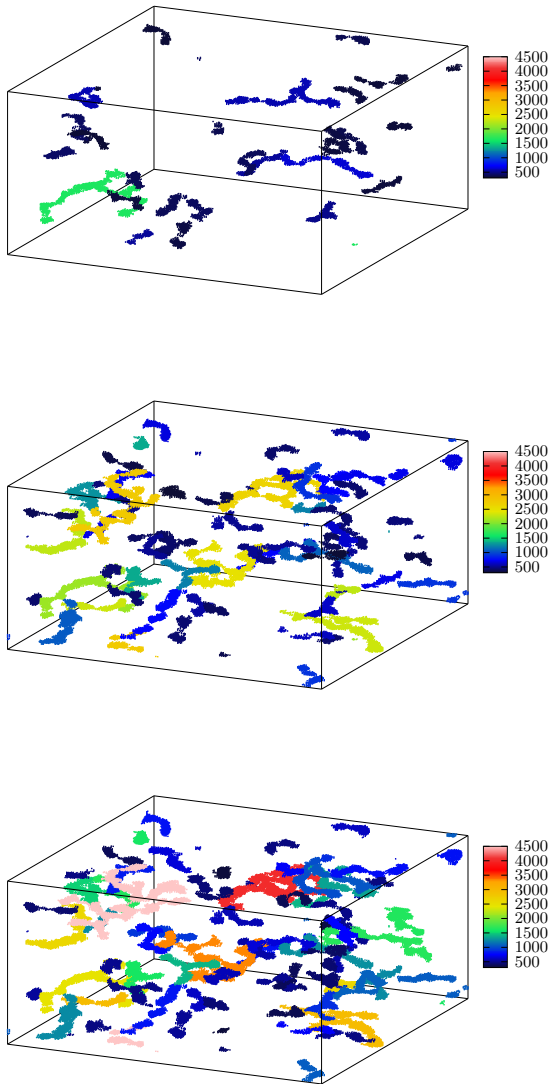


FIG. 2. (color online) Clusters containing more than 300 active sites at three different times. From top to bottom: $t = 5$, 10, and 15 ps. The system temperature is $T = 700$ K. Cluster size is indicated by grey (color) scale

tom), where the cluster size M is plotted against the cluster length l on a log-log scale for the same times. Since these quantities are related through $M \sim l^{d_f}$, the data clearly show that, at short times, most clusters are nearly one-dimensional. At longer times, two distinct populations emerge: one consisting of small, quasi-one-dimensional clusters, and another corresponding to larger, branched clusters characterized by a fractal dimension close to $d_f \simeq 1.7$. Straight lines with slopes 1 and 1.7 are included as guides to the eye.

To assess whether the ion-conducting pathways are ultimately determined by the rigid silicon-oxygen back-

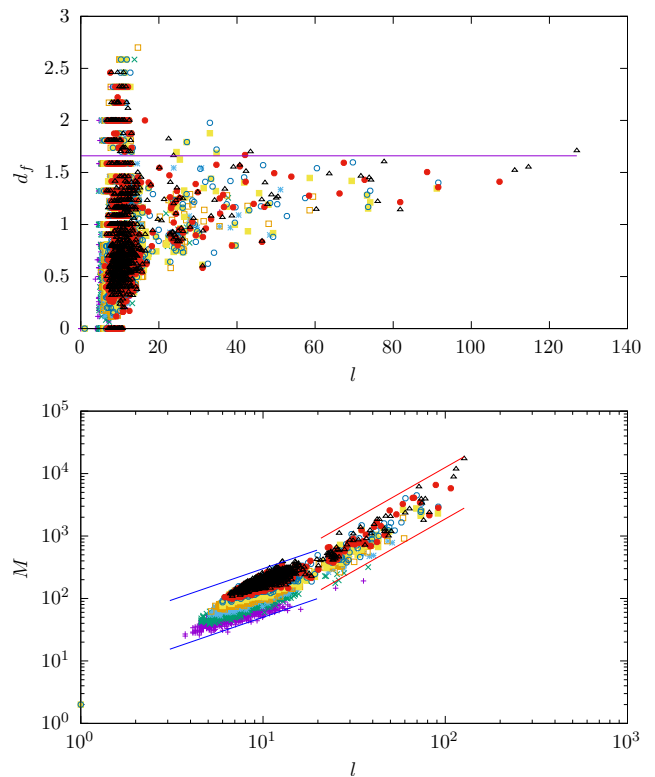


FIG. 3. (color online) Cluster properties at $T = 700$ K. Top panel: box-counting fractal dimension as a function of cluster length for all clusters at different times: $t = 1$ (violet plus), 2 (green cross), 4 (light-blue star), 6 (orange empty square), 10 (yellow filled square), 15 (blue empty-circle), 20 (red filled circle), 30 (black empty triangle) ps. The horizontal line indicates $d_f = 1.7$. Bottom panel: cluster size versus cluster length for the same times. The lines with slopes 1 (left) and 1.7 (right) are shown as guides to the eye.

bone that emerges at the glass transition, we also analysed the evolution of active-site clusters at $T = 1100$ K, i.e., close to T_g . This comparison allows us to disentangle the role of structural arrest from purely dynamical effects in shaping the geometry of the conduction pathways. Fig. 4 shows, using the same analysis performed at $T = 700$ K, the statistical properties of active-site clusters at $T = 1100$ K and times $t = 0.10, 0.15, 0.40, 0.80, 1.20, 2.50, 5.00$ and 7.50 ps. Although the time evolution is significantly much faster at this higher temperature, the results again indicate that at short times the conducting pathways are predominantly one-dimensional, while at longer times larger structures emerge, characterized by fractal dimension $d_f \simeq 1.7$. Notably, at the longest times considered at $T = 1100$ K, small clusters reappear. This behaviour indicates that the silicate network has begun to lose memory of its initial condition; consistent with the pronounced decay of the incoherent scattering function observed after a few picoseconds at this temperature [25, 27].

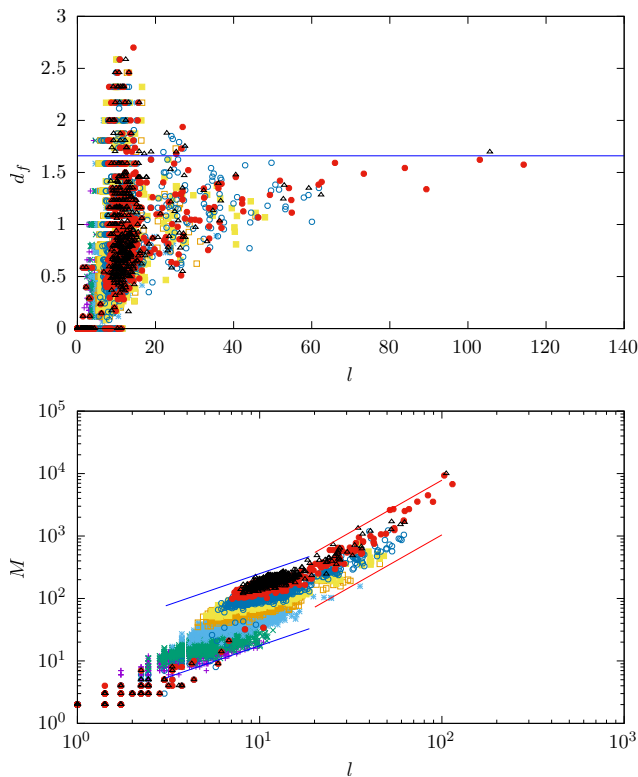


FIG. 4. (color online) Cluster properties at $T = 1100K$. Top panel: box-counting fractal dimension as a function of cluster length for times $t = 0.10$ (plus violet), 0.15 (cross green), 0.40 (star light-blue), 0.80 (empty-square orange), 1.20 (filled-square yellow), 2.50 (empty-circle blue), 5.00 (filled-circle red), and 7.50 (empty-triangle black) ps. The horizontal line indicates $d_f = 1.7$. Bottom panel; cluster size versus cluster length for the same times. Straight lines with slopes slopes 1 (left) and 1.7 (right) are shown as guides to the eye.

Summary and conclusions.-

We have investigated ionic transport in a lithium metasilicate glass below and near the glass-transition temperature by combining mobility-resolved dynamics with a real-space characterization of ion-conducting pathways. Ensemble-averaged velocity autocorrelation functions rapidly decorrelate and fail to capture dynamic heterogeneity, whereas single-ion analysis reveals short-lived episodes of nearly collinear motion. By mapping the regions explored by lithium ions, we show that ion-conducting pathways are quasi one-dimensional at short times, with a fractal dimension close to unity, and progressively evolve into larger branched structures characterized by a robust fractal dimension $d_f \simeq 1.7$. This geometry persists as long as the silicate backbone remains structurally arrested, while near T_g the loss of structural memory leads to the reappearance of small clusters. Altogether these results provide microscopic evidence that ionic transport in non-crystalline solids proceeds through

transient fractal pathways, offering a structural basis for the high-frequency regime of the Universal Dielectric Response observed in ion-conducting glasses.

Acknowledgements.- This work was supported by the Universidad Nacional del Sur, PGI 24/Q146, the Universidad Nacional de Mar del Plata, 15/E1040, Agencia Nacional de Promoción Científica y Tecnológica (AN-PCyT), PICT 2021-00288, and Consejo Nacional de Investigaciones Científicas y Técnicas (CONICET), PIP-21 GI11220200100317CO. The authors are Research Fellows at CONICET, Argentina.

-
- [1] A. Jonscher, *Nature* **267**, 673 (1977).
 - [2] C. Balbuena and M. A. Frechero, *Computational Materials Science* **215**, 111821 (2022).
 - [3] B. Roling, *J. Non-Cryst. Solids* **244**, 34 (1999).
 - [4] A. P. Sokolov, A. Kisliuk, V. N. Novikov, and K. Ngai, *Phys. Rev. B* **63**, 172204 (2001).
 - [5] C. Balbuena, M. A. Frechero, and R. Montani, *Journal of Non-Crystalline Solids* **369**, 17 (2013).
 - [6] R. Montani, C. Balbuena, and M. A. Frechero, *Solid State Ionics* **209**, 5 (2012).
 - [7] M. A. Frechero, L. Padilla, H. Martín, and J. L. Iguain, *EPL* **103**, 36002 (2013).
 - [8] B. Roling, M. Meyer, A. Bunde, and K. Funke, *Journal of Non-Crystalline Solids* **226**, 138 (1998).
 - [9] K. Funke, R. D. Banhatti, L. G. Badr, D. M. Laughman, and H. Jain, *J. Electroceram.* **34**, 4 (2015).
 - [10] W. K. Lee, J. F. Liu, and A. S. Nowick, *Phys. Rev. Lett.* **67**, 1559 (1991).
 - [11] A. S. Nowick, A. Vaysleyb, and W. Liu, *Solid State Ionics* **105**, 121 (1998).
 - [12] J. Habasaki, K. L. Ngai, and Y. Hiiwatari, *Phys. Rev. E* **66**, 021205 (2002).
 - [13] F. O. Sanchez-Varretti, J. L. Iguain, J. M. Alonso, and M. A. Frechero, *Nano Express* **5**, 025015 (2024).
 - [14] J. M. Alonso, F. O. Sanchez-Varretti, and M. A. Frechero, *Eur. Phys. J. E* **44**, 88 (2021).
 - [15] Y. Ida, *Phys. Earth Planet. Inter.* **13**, 2 (1976).
 - [16] J. Habasaki, I. Okada, and Y. Hiwatari, *Mole. Simul.* **9**, 49 (1992).
 - [17] J. Habasaki, I. Okada, and Y. Hiwatari, *Mole. Simul.* **10**, 19 (1993).
 - [18] J. Habasaki and Y. Hiiwatari, *Phys. Rev. E* **65**, 021604 (2002).
 - [19] S. Plimpton, *J. Comput. Phys.* **117**, 1 (1995).
 - [20] C. Balbuena, R. Montani, and M. A. Frechero, *Physica A Stat. Mech. Appl.* **432**, 400 (2015).
 - [21] J. J. Erpenbeck and W. W. Wood, *Phys. Rev. A* **32**, 412 (1985).
 - [22] A. Fukumoto, A. Ueda, and Y. Hiwatari, *Solid State Ionics* **3/4**, 115 (1981).
 - [23] M. Hokazono, A. Ueda, and Y. Hiwatari, *Solid State Ionics* **13**, 151 (1984).
 - [24] R. D. Banhatti and A. Heuer, *Phys. Chem. Chem. Phys.* **3**, 5104 (2001).
 - [25] A. Heuer, M. Kunow, M. Vogel, and R. D. Banhatti, *Phys. Rev. B* **66**, 224201 (2002).
 - [26] F. Kargl, A. Meyer, M. M. Koza, and H. Schober,

Phys. Rev. B **74**, 014304 (2006).

[27] C. Balbuena, C. Brito, and D. Stariolo, J. Phys.: Condens. Matter **26**, 155104 (2014).